POLARIZATION OPTICAL STUDIES AT LARGE STRAINS

A. Ya. Aleksandrov, M. Kh. Akhmetzyanov,
G. N. Albaut, and V. N. Baryshnikov

The questions of polarization optical study of the problems of nonlinear elasticity and plasticity theory with large strains are discussed. In one case transparent models made from rubberlike materials are used for the study, in the other case the photoelastic coating method is used [1, 2]. In both cases polyurethane rubber of the SKU-6 type [3] is used as the piezo-optical material. Studies of both elastic [4] and plastic [5] strains have already been made using this material. However linear strain theory was used in [4, 5] to analyze the optical patterns. In the present study we propose a technique based on the theory of strain for rubberlike materials in the Mooney-Rivlin variant. This approach is used to study the optical and mechanical properties of SKU-6 and to examine the questions of analysis of the optical patterns, and examples of such studies are presented.

NONLINEAR PHOTOELASTICITY

Polarization optical studies [3, 4, 6-9] of the stress-strain state of transparent models for finite elastic strains (nonlinear photoelasticity) have established that for materials of the transparent rubber type the Wertheim law in the following form holds for large strains

$$\delta = c_\sigma h_0 \lambda_3 (\sigma_1 - \sigma_2) \tag{1.1}$$

Here c_σ is the optical constant; σ_1 and σ_2 are the principal true stresses; h_0 is the plate thickness in the undeformed state; $\lambda_j = l_j / l_{j,0}$ ($j = 1, 2, 3$) are the principal elongation ratios; $l_{j,0}$ and l_j are some dimension prior to and after deformation. The plate is illuminated along λ_3.

In this case, in contrast with the corresponding law for small strains, we take into account only the change of the element thickness in the strain process. For elastic strain of isotropic materials the directions of the principal stresses, principal elongations, and optical axes coincide and can be found by constructing the isocline field.

To obtain the connection between the optical path difference δ and the strains of models made from incompressible materials (which SKU-6 may be considered) we use the representation of the elastic potential in the form of the Mooney series [6, 7, 10, 11]

$$W = W_2 + W_4 + \ldots\ldots + W_{2n} \tag{1.2}$$

Here

$$W_{2n} = A_{2n}(\lambda_1^{2n} + \lambda_2^{2n} + \lambda_3^{2n} - 3) + B_{2n}(\lambda_1^{-2n} + \lambda_2^{-2n} + \lambda_3^{-2n} - 3)$$

where A_{2n}, B_{2n} are constants of the material.

The stresses are found from the expressions

$$\sigma_j = \lambda_j \partial W / \partial \lambda_j + \sigma_0, \text{ where } \sigma_0 = {}^1/_3 (\sigma_1 + \sigma_2 + \sigma_3) \tag{1.3}$$

We take only two terms of the series (1.2). Then for the plane stress state with account for the incompressibility condition

$$\lambda_1 \lambda_2 \lambda_3 = 1 \tag{1.4}$$

we obtain

Novosibirsk. Translated from Zhurnal Prikladnoi Mekhaniki i Tekhnicheskoi Fiziki, Vol. 10, No. 5, pp. 89-99, September-October, 1969. Original article submitted May 26, 1969.

© 1972 Consultants Bureau, a division of Plenum Publishing Corporation, 227 West 17th Street, New York, N. Y. 10011. All rights reserved. This article cannot be reproduced for any purpose whatsoever without permission of the publisher. A copy of this article is available from the publisher for $15.00.

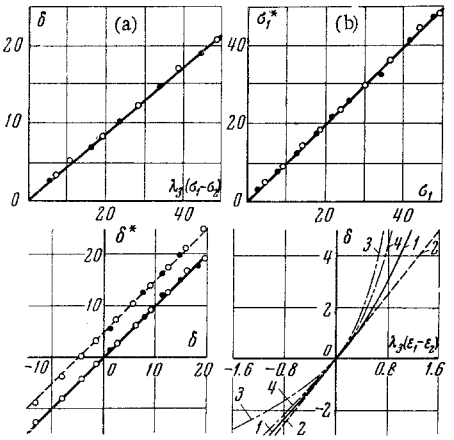

Fig. 1

$$\sigma_1 = 2(A_2 + B_2\lambda_2^2)(\lambda_1^2 - \lambda_3^2) + 4(A_4 + B_4\lambda_2^4)(\lambda_1^4 - \lambda_3^4)$$
$$\sigma_2 = 2(A_2 + B_2\lambda_1^2)(\lambda_2^2 - \lambda_3^2) + 4(A_4 + B_4\lambda_1^4)(\lambda_2^4 - \lambda_3^4) \quad (1.5)$$

Substituting (1.5) into (1.1), we find

$$\delta = c_\sigma h_0 \lambda_3 [2(A_2 + B_2\lambda_3^2)(\lambda_1^2 - \lambda_2^2) + 4(A_4 + B_4\lambda_3^4)(\lambda_1^4 - \lambda_2^4)] \quad (1.6)$$

The relations (1.1), (1.4)–(1.6) were verified experimentally on specimens of the SKU-6 material. This clear rubber deforms elastically up to relative elongations of the order of hundreds of percent, yields over this entire interval a clear interference pattern, does not mainfest creep effects at room temperature, does not have initial and residual optical path differences, and is similar in its mechanical properties to certain of the rubbers used industrially.

Specimens in the form of strips were prepared for uniaxial tension, models in the form of a cross whose ends were split into narrow strips to create a uniform stress state in the working zone of the model were used for the biaxial tension tests. The compression tests were made on specimens of rectangular form under plane strain conditions. To this end the plate was placed between two plexiglass sheets, joined using four bolts, which made it possible to alter the magnitude of the transverse strain. The sheet surfaces were lubricated with glycerine to reduce friction.

For the SKU-6 material the constants, determined from biaxial tension tests and analyzed by the method of least squares, were as follows: $A_2 = 8.8$ kg/cm^2, $B_2 = -0.66$ kg/cm^2, $2A_4 = -0.51$ kg/cm^2, $2B_4 = 0.38$ kg/cm^2. The stress ratio σ_2/σ_1 in these tests varied from 0.1 to 1.0.

It was noted that the relationship between the constants can be considered constant for different lots of the SKU-6 rubber, i.e., to determine the mechanical characteristics of the lot it is sufficient to determine the single constant A_2 in uniaxial testing of a calibration specimen.

The results of verification of (1.1) for the test material are shown in Fig. 1a, above. Here and hereafter the dark and light circles denote the experimental points for uniaxial and biaxial stress states respectively. The upper partion of Fig. 1b shows results of the check of (1.5). Here the vertical scale is the true value of the principal stresses σ_1^*, calculated from the measured forces, and the horizontal scale is the value of σ_1 in kg/cm^2, calculated from the measured extensions with the aid of (1.5). The tests were made for $0.5 \leq \lambda \leq 2.5$. In the process of these tests the optical path differences and transverse strains of the specimens were also recorded. This made possible a check at the same time of the relations (1.4) and (1.6). The SKU-6 material was practically incompressible. The results of the check of (1.6) are represented by the points and continuous curve in the lower part of Fig. 1a; the vertical scale is the experimentally measured value of the optical path difference δ^*, fringes/mm, and the horizontal scale is the value of δ, fringes/mm, calculated with the aid of (1.6). We see that this relation approximates well the optical strain relation over the entire range of strains investigated ($0.5 \leq \lambda \leq 2.5$).

Let us establish the possibility of applicability of relations which are simpler than (1.6). It follows from [3, 4] that for the SKU-6 material we can with adequate accuracy consider that the path difference is proportional to the difference of the principal Cauchy strains, i.e.,

$$\delta = c_\varepsilon h_0 \lambda_3 (\varepsilon_1^k - \varepsilon_2^k) = c_\varepsilon h_0 \lambda_3 (\lambda_1 - \lambda_2) \quad (1.7)$$

The points through which the dashed line, shifted relative to the coordinate origin (Fig. 1a, below), passes are plotted from the results of the experiments and calculations using (1.7). We see that (1.7) approximates quite well the optical strain relation over a large strain interval.

It follows from comparison of (1.7) and (1.6) that in this case the quantity

$$k = 2(A_2 + B_2\lambda_3^2)(\lambda_1 + \lambda_2) + 4(A_4 + B_4\lambda_3^4)(\lambda_1 + \lambda_2)(\lambda_1^2 + \lambda_2^2)$$

must be nearly constant. The calculations showed that for the values of the coefficients A_2, B_2, A_4, B_4 found for SKU-6 in the interval investigated the quantity k actually varies only slightly. For materials with a different relationship of these coefficients, the quantity k differs significantly from a constant and therefore

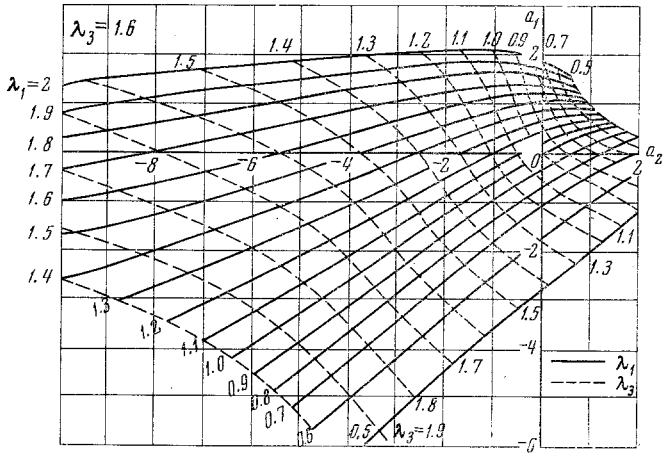

Fig. 2

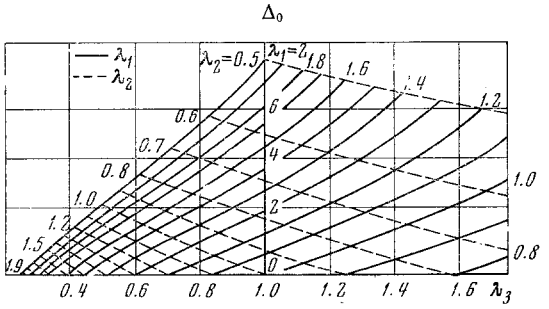

Fig. 3

(1.7) may lead to errors. Figure 1b, below, shows our reduction of the data for rubber obtained in [8] for the uniaxial stress state. Here the horizontal scale is the value of $\lambda_3(\varepsilon_1-\varepsilon_2)$. In plotting curve 1 the values of ε_1 and ε_2 corresponded to Cauchy strains, 2 is for Green strains, 3 is for Almansi strains, 4 is for Hencky strains. For this rubber the optical strain relation for the uniaxial stress state is approximated well by a linear relationship between the optical path difference and the difference of the Green principal strains

$$\delta = c_\varepsilon h_0 \lambda_3 (\varepsilon_1^G - \varepsilon_2^G) \qquad (1.8)$$

We see from these examples that linear relations between δ and the difference of the principal strains are not universal, and for a definite choice of the strain measure are suitable only for a material of a given sort. In using these relations it is necessary to exercise considerable care, since for some of them it is found that the "optical constant" c_ε is a function of the form of the stress state.

Thus, on the basis of measurements with normal transillumination of a plane stress model we can determine the differences of the principal running forces $\lambda_3\sigma_1 - \lambda_3\sigma_2$ and the directions of the principal stresses (strains).

Let us examine some techniques for separating the stresses:

a) Integration of the Equilibrium Equations for the Plane Problem. We have

$$\partial(\lambda_3\sigma_x) / \partial x + \partial(\lambda_3\tau_{xy}) / \partial y = 0 \qquad (x,\ y) \qquad (1.9)$$

Expressions (1.9) make it possible to find in the usual way the individual values of the principal running forces $\lambda_3\sigma_1$ and $\lambda_3\sigma_2$. To find the true stresses σ_1 and σ_2 and the quantities λ_1, λ_2, λ_3 we use in addition the coupling equations (1.5) and the incompressibility conditions (1.4). The solution of the resulting system of equations is carried out with the aid of the nomogram shown in Fig. 2. Here the axes are the values of the reduced principal running forces $a_1 = \lambda_3\sigma_1/2A_2$ and $\lambda_2 = \lambda_3\sigma_2/2A_2$, found by integration of (1.9). The intersection of the coordinate lines defines λ_1 and λ_3, knowing which we can easily find λ_2 from (1.4) and σ_1, σ_2. In constructing the nomogram we used the relations between the constants presented above for SKU-60. We note that a similar technique was used in [4], however there the connection between the stresses and the strains is written in the form of the generalized Hooke's law.

b) Transverse Strain Measurement. If in the experimental process, in addition to normal transillumination of the model we also measure its transverse strains, then finding the individual values of the strains and stresses reduces to the solution of the system of equations (1.5), (1.1), (1.4) which can be accomplished when using the SKU-6 material with the aid of the nomogram shown in Fig. 3. Here the

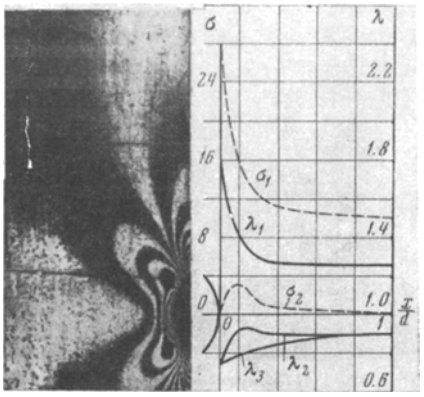

Fig. 4

horizontal axis is the measured value of λ_3, the vertical axis is the reduced path difference $\Delta_0 = \delta/c_\sigma A_2 h_0$, the point of intersection of the coordinate lines defines λ_1 and λ_2, knowing which we can calculate the stresses σ_1 and σ_2 using (1.5).

c) Oblique Transillumination of the Model. If oblique transillumination is accomplished in the plane of one of the principal stresses, then the path difference δ_k will be connected with the principal stresses by the relation

$$\delta_k = c_\sigma h_0 \lambda_3 (\sigma_1 - \sigma_2 \cos^2 \theta) / \cos \theta \qquad (1.10)$$

Here θ is the transillumination angle.

Combining with this equation the basic photoelasticity law (1.1) and solving these equations for the principal forces, we find

$$\lambda_3 \sigma_1 = (\delta_k \cos\theta - \delta \cos^2 \theta)/h_0 c_\sigma \sin^2\theta$$
$$\lambda_3 \sigma_2 = (\delta_k \cos\theta - \delta)/h_0 c_\sigma \sin^2\theta \qquad (1.11)$$

The nomogram shown in Fig. 2 can be used to find the values of the principal stresses and the principal extension ratios.

As an example we consider stretching of a plate with a circular (prior to stretching) hole in the center. Figure 4 shows the fringe pattern and curves of the principal true stresses in the cross section of the plate, obtained by numerical integration of the equations of equilibrium. The magnitude of the true stress in the uniform stress state zone was $\sigma_0 = 11$ kg/cm^2.

We also present the results of a study of stretching of a wide plate which is rigidly clamped along two sides. The fringe partten (continuous curves on which the numerals denote the fringe order) and the isoclines (dashed) are shown in Fig. 5 (direction of motion indicated by the arrow). Also shown are the curves of the extension ratios and stresses (kg/cm^2) in the cross section of the plate. The separation of the stresses and strains was accomplished using the same technique as in the preceding example.

STUDY OF LARGE STRAINS USING PHOTOELASTIC COATINGS

The study of large plastic strains using photoelastic coatings has frequently been made [12, 13] with the aid of plasticized epoxy resins, which manifest significant relaxation and instability of the physical and mechanical properties. In our studies we used for this purpose the SKU-6 polyurethane rubber whose properties were described above. Several techniques for applying the coating to the surface of the part were tried.

a) Bonds using adhesives of the PU-2, leuconate, and certain other types fail at relative extensions in the plane of the bond on the order of 10-20%. Adhesives Nos. 88 and 4 provide compatible operation of the coating and the part up to strains on the order of 100%, however they react with the SKU-6 during polymerization and alter somewhat the optical strain characteristics of this material.

b) Direct polymerization of SKU-6 on the surface of the part provides strong adhesion of the coating with the metal right up until failure of the part. The disadvantages are the difficulty in polymerization of the coatings on a curved surface and complications associated with the necessity for "conditioning" the material to give it stable properties. The conditioning involves applying several arbitrary loading cycles to the material, which can be done by stretching the SKU-6 plates several times by hand. The conditioning of the coating must be accomplished by means of several compression cycles in the direction normal to the surface.

c) Bonding flat rubber sheets to the surface using an adhesive in the form of the SKU-6 composition prepared for polymerization avoids the drawbacks of the two preceding techniques and is used to obtain coatings of thickness one millimeter or more on flat and curved surfaces. The contouring around the curved surfaces does not cause any marked optical effect and the effect of the "unconditioned" adhesive layer is quite small for the coating thickness mentioned above. The drawback of this and the previous technique is the fact that polymerization of the rubber is accomplished at a high temperature (120° C).

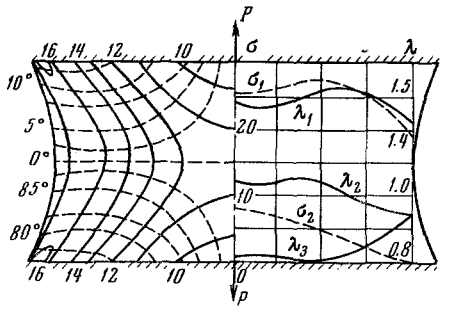

Fig. 5

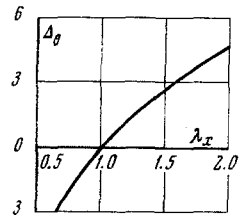

Fig. 6

The principal strain directions and the extension ratio function (1.6) are determined from the data of normal transillumination of the photoelastic coatings. For separate determination of the strains we can use the methods discussed above for measuring the transverse strains, oblique transillumination, and also the coating slicing technique. In this case we first measure the optical path difference and the directions of the optical axes in the continuous coating and then the coating is sliced (using a razor blade, for example) through the entire depth at the section being studied. By measuring the optical path difference at the edge of the slice

$$\Delta_0 = \delta / c_\sigma A_2 h_0 \qquad (2.1)$$

we can with the aid of the calibration curve (Fig. 6), obtained in simple extension and compression, determine the extension ratio λ_x in the direction of the slice. The value of λ_x is connected with the extension ratios λ_1 and λ_2 by the relation

$$\lambda_x^2 = {}^1/_2\ (\lambda_1^2 + \lambda_2^2) + {}^1/_2\ (\lambda_1^2 - \lambda_2^2) \cos 2\alpha \qquad (2.2)$$

Combining with (2.2) the data obtained in studying the continuous coating, and also the incompressibility condition, we obtain the complete system of equations for finding λ_1, λ_2, λ_3.

The nomogram of Fig. 7 is constructed to facilitate the solution of this system. Here the values of λ_x (left axis) and α (right axis) are laid off along the vertical axes and the resulting points are connected by a straight line. The point of intersection of this line with the corresponding line $\Delta_0 = \delta / c_\sigma A_2 h_0 = \text{const}$ defines the extension ratio λ_1.

The nomogram shows an example for the case in which $\lambda_x = 1.5$, $\alpha = 65°$, $\Delta_0 = 0.8$. Projecting the resulting point on the λ_1 axis along the radial lines, we find that in this case $\lambda_1 = 1.9$. To find λ_2 we use the expression which follows from (2.2)

$$\lambda_2^2 = (\lambda_x^2 - \lambda_1^2 \cos^2 \alpha) / \sin^2 \alpha \qquad (2.3)$$

The quantity λ_3 can be found from the known λ_1 and λ_2 using the incompressibility condition (1.4). From the resulting extension ratios we can calculate the principal components of the logarithmic strain tensor, which is usually used to describe the strain state for large plastic strains

$$\varepsilon_j = \ln \lambda_j \quad (j = 1, 2, 3)$$

Here the ε_j are the logarithmic strains.

To determine the stresses from the measured strains we can use the method of reproduction of the strain history [14, 15]. The basis for this method is the hypothesis of macrophysical determinability [16]. Here, to determine the stresses at the point of the part in question it is necessary to establish the strain tensor component variation process and then reproduce this process on uniformly strainable specimens of finite dimensions, for example on thinwall tubes subjected to simultaneous action of tension, torsion, and internal pressure. In the process of this reproduction it is necessary to establish the forces required for the reproduction, knowing which we can easily find the magnitudes of the stress tensor components in the specimen. In this way we can define a specimen loading process which on the basis of the hypothesis of macrophysical determinability will be equivalent to the loading process at the point in question of the nonuniformly stressed part.

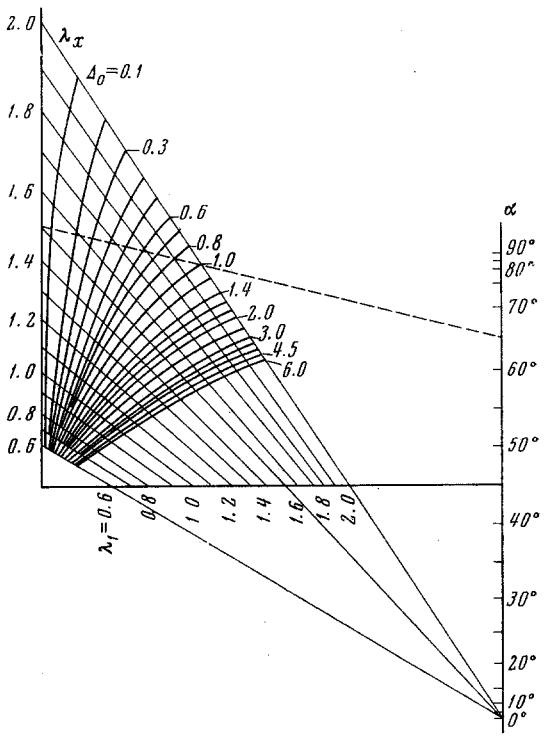

Fig. 7

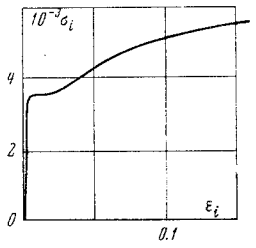

Fig. 8

In those cases in which the unloading of the material can be described sufficiently exactly by Hooke's law, we can use the unloading method [17] to determine the stresses. In this case the process of complete unloading of the part must be carried out so that creep effects do not show up ("instantaneous" unloading) and plastic strains do not arise. From the measured elastic strains with the aid of Hooke's law we find the stresses present in the part when it is loaded (working stresses). Complete unloading of the part is accomplished by removing all the forces and other factors acting with subsequent slicing of the part into elementary cubes or bars. It is obvious that the part must be free of residual stresses prior to loading, and the sequence and time for complete unloading must ensure satisfaction of linear unloading conditions.

Another version of this scheme involves determining experimentally the residual stress tensor in the model after "instantaneous" removal of the forces and, in addition, determination of the stress tensor during elastic strain of the model by the same loads. The latter is accomplished either by the analytic methods of elasticity theory or by the known techniques for modeling elastic problems. In this case the model must be geometrically similar to the full-scale part at the moment immediately preceding its unloading. The practical realization of this scheme for finding the stresses became possible after sufficiently general schemes were found for studying the residual stresses in bodies of arbitrary form [18-19].

If flow theory is used as the basis for the study, we use the following relations to find the stresses:

$$\sigma_j = \sigma_0 + 2\sigma_i (\varepsilon_j^{\cdot} - \varepsilon_0^{\cdot}) / 3\varepsilon_j^{\cdot} \qquad (j = 1, 2, 3) \tag{2.4}$$

Here σ_i is the stress intensity, ε_i is the strain intensity rate, ε_j are the principal strain rates, and ε_0 is the average strain rate.

The stress intensity is found with the aid of its dependence on the strain ratio e. For the monotonic loading case, when in the deformation process the principal strain tensor components increase in proportion to a single parameter and the principal strain directions remain fixed relative to the material fibers of the body, e is defined by the intensity of the principal logarithmic strains

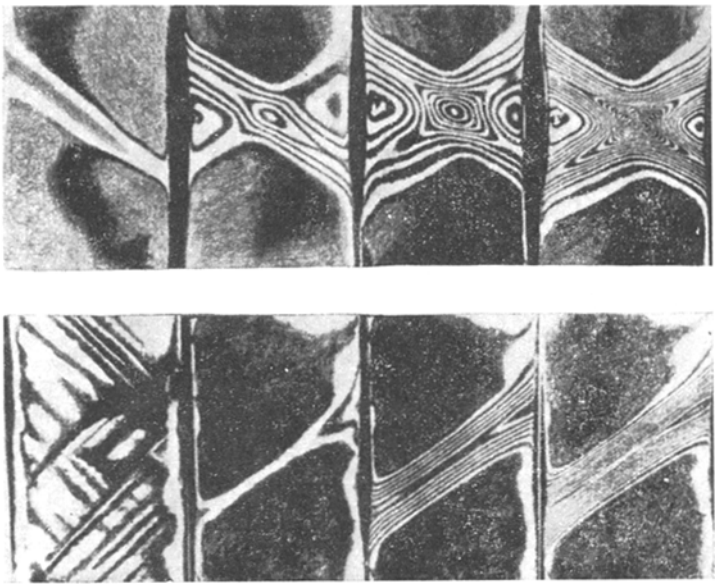

Fig. 9

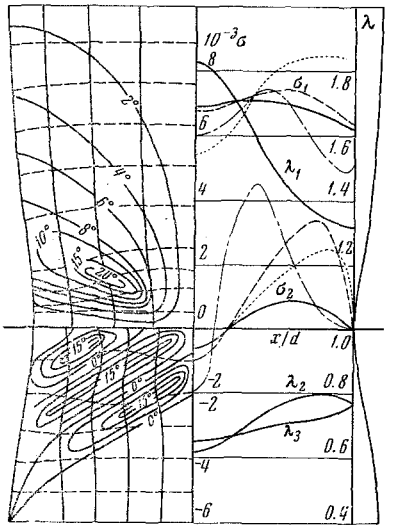

Fig. 10

$$e = \frac{\sqrt{3}}{2}\left[\left(\ln\frac{\lambda_1}{\lambda_2}\right)^2 + \left(\ln\frac{\lambda_2}{\lambda_3}\right)^2 + \left(\ln\frac{\lambda_3}{\lambda_1}\right)^2\right]^{1/2} \tag{2.5}$$

In this case of nonmonotonic loading the following expression is used to calculate the strain ratio:

$$e = \int_0^t \varepsilon_i^{\cdot}\, dt \tag{2.6}$$

In determining the stresses with the aid of (2.4), the entire loading process must be divided into several stages, and a polarization-optical study must be made for each loading stage. In (2.4) and (2.6) we can substitute in place of the strain rates their increments, obtained from the difference of the deformations of two neighboring stages.

In studying plane plasticity problems, just as in the case of small strains [20], we can find the stresses on the basis of separately taken plasticity theory hypotheses. Thus, if the principal strain (or strain rate) directions are obtained experimentally, on the basis of the corresponding hypotheses these directions can be taken as the principal stress directions. Then the process of finding the magnitudes of the stresses in the plastic zone reduces to numerical integration of the equilibrium equations (1.9) for the plane problem.

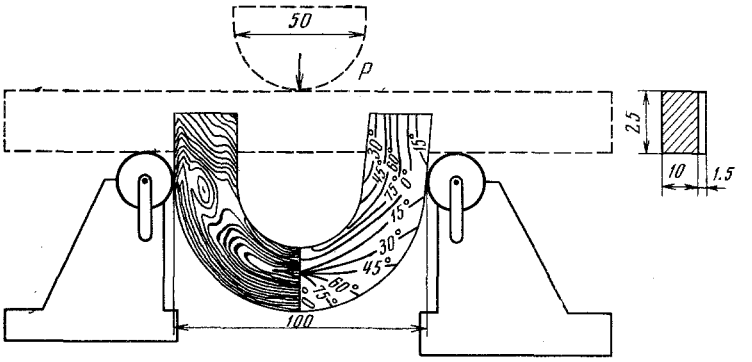

Fig. 11

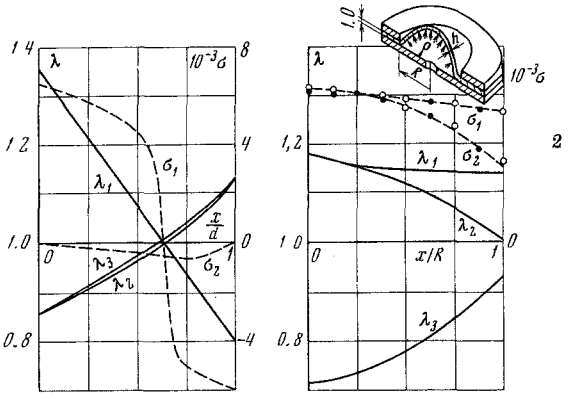

Fig. 12

Similarly, if the magnitudes of the strain (or the maximal shear) intensities are found experimentally, on the basis of the single hardening curve hypothesis we can find the stress intensity (or the maximal tangential stresses). Finding the individual magnitudes of the stresses again reduces to numerical integration of the equations of equilibrium for the plane problem. However (2.4) and the hypotheses on which they are based (coaxiality of the directions of the principal stresses and strain increments, single hardening curve) are valid only for simple (or sufficiently close to simple) strain processes.

Let us examine some illustrative examples.

a) Stress and strain state of the neck of a plane specimen in tension (cross section 100 × 10 mm, steel, stress-strain curve shown in Fig. 8, where σ_i is in kg/cm^2).

In testing a large number of specimens, approximately equal numbers of cases with the development of symmetric and inclined necks were observed. The characteristic fringe patterns for gradual development of such necks are shown in Figs. 9a and b, respectively. The isocline fields and the trajectories of the total principal strains and their increments for the symmetric neck, and also the curves of the principal extension ratios in the minimal cross section of this neck are shown in Fig. 10 (continuous curves). Also shown are the curves of the principal stresses σ_1 and σ_2. These stresses were determined on the basis of the hypothesis on coincidence of the directions of the principal stresses and the principal strain increments (dash-dot) with the aid of the equations of the deformational plasticity theory (continuous curves), with the aid of the equations of flow theory (dashed), and with the aid of the unloading method (points). In the latter case the stresses were found by summation of the residual stresses, measured using the strip slicing technique [17] in the necked specimen after unloading, together with the stresses found by the photoelasticity method in an elastic model fabricated from the ED-6M material with satisfaction of geometric similarity to the full-scale part at the moment of unloading.

The calculations showed that in all cases the maximal values of the stress intensities are reached at points lying at the center of the neck, which is where failure of the specimen begins. The realization of the technique for reproduction of the deformation strain history in this example involves difficulty in obtaining the required uniform stress state with such large strains.

b) Bending flat specimen made from soft steel around a mandrel. The loading scheme, fringe pattern, and isocline pattern are shown in Fig. 11. Figure 12, left, shows the strain distribution in the middle section of the specimen and the normal stress curves, obtained on the basis of the equations of deformational plasticity theory.

c) Drawing axisymmetric shell from a round plate (red copper) loaded by hydrostatic pressure. Figure 12, right, shows the stress curves in the meridional section of the shell, obtained with the aid of the equations of equilibrium (light circles) and on the basis of the equations of the strain theory of plasticity (dark circles) from the measured strains λ_i.

LITERATURE CITED

1. A. Ya. Aleksandrov, "A possible scheme for applying the photoelastic method to the study of plane elasto-plastic problems," Tr. Novosib. in ta inzh. zh d. transp. No. 8 (1952).
2. A. Ya. Aleksandrov and M. Kh. Akhmetzyanov, "Study of elasto-plastic problems by the photoelastic coating method," Proceedings of 2nd All-Union Conference on Theoretical and Applied Mechanics; Solid State Mechanics [in Russian], No. 3 (1966).
3. B. M. Gorelik and G. I. Fel'dman, "The SKU-6 optically active rubber," Kauchuk i rezina, No. 12 (1963).
4. B. M. Gorelik and G. I. Fel'dman, "Study of stresses in plane model of rubber "O" ring," Kauchuk i rezina, No. 4 (1963).
5. L. A. Sosnovskii and L. I. Byakov, "Determining large strains by the photoelastic coating method," Zavosdk. laboratoriya, No. 11 (1968).
6. Rheology [Russian translation], Izd vo inostr. lit., Moscow (1953).
7. L. R. G. Treloar, Physics of Rubber Elasticity [Russian translation], Izd-vo inostr. lit. Moscow (1963).
8. A. Angioletti, "Photoelastic study of rubber products," Khimiya i tekhnol. polimerov, No. 4 (1957).
9. A. J. Durelli and A. P. Mulzet, "Large strain analysis and stresses in linear materials," Proc. Amer. Soc. Civil Engrs. Engng Mech. Division, Vol. 91, No. EM3, pt. 1, 2 (1965).
10. S. D. Ponomarev, V. L. Biderman, K. K. Likharev, et al., Stress Analysis in Machine Design, Vol. 2 [in Russian], Gostekhizdat, Moscow (1958).
11. A. E. Green and J. E. Adkins, Large Elastic Deformations and Nonlinear Continuum Mechanics [Russian translation], Mir, Moscow (1965).
12. V. K. Vorontsov, P. I. Polukhin, N. I. Prigorovskii, S. I. Sokolov, and N. A. Shchegolevskaya, "Optically sensitive coatings for studying plastic strains," collection: Strength Problems in Machine Design [in Russian], Izd vo AN SSSR, Moscow No. 8 (1962).
13. V. K. Vorontsov and P. I. Polukhin, "Application of the optically sensitive coating method to the study of pressure working of metals," collection: Polarization Optical Method for Studying Stresses: Proceedings of 5th All Union Conference, 1964 Izd vo LGU, Leningrad (1966).
14. A. Ya. Aleksandrov and M. Kh. Akhmetzyanov, "Experimental study of stresses and strains in inelastic bodies," Summaries of Reports to the 3rd All-Union Convention on Mechanics [in Russian], Nauka, Moscow (1968).
15. A. Ya. Aleksandrov and M. Kh. Akhmetzyanov, "Study of inelastic problems by reproducing the strain history," Dokl. AN SSSR, Vol. 186, No. 1 (1969).
16. A. A. Il'yushin, Plasticity [in Russian], Izd vo AN SSSR, Moscow (1963).
17. M. Kh. Akhmetzyanov, "Stress determination by unloading method in simulation of plasticity and elasticity prolbems," Prikl. mekhan. [Sovient Applied Mechanics], No. 2 (1968).
18. M. Kh. Akhmetzyanov, "Study of residual stress state of cylindrical bodies, " Zavodsk. laboratoriya, No. 1 (1967).
19. M. Kh. Akhmetzyanov, "Scheme for studying residual stresses in bodies of arbitrary form," Tr. Novosib. in ta inzh. zh. d. transp., No. 62 (1967).
20. A. Ya. Aleksandrov and M. Kh. Akhmetzyanov, "Study of plane elasto-plastic problems using photo-elastic coatings," PMTF, Vol. 2, No. 6 (1961).